Earthquake Geotechnical Engineering for Protection and Development of Environment and Constructions – Silvestri & Moraci (Eds)
© 2019 Associazione Geotecnica Italiana, Rome, Italy, ISBN 978-0-367-14328-2

Seismic response analysis of offshore bridges considering site liquefaction

Y. Gu, Z.Y. Huang, L. Cai & W.D. Zhuo
Fuzhou University, Fuzhou, Fujian, China

ABSTRACT: This paper investigates the influence of site liquefaction on seismic responses of an offshore bridge. A three-dimensional saturated soil-bridge model and the same model without consideration of saturated soil were modeled on the platform of OpenSeeS. The response results of the two models have been compared and discussed. The results showed that liquefied sites had an obvious amplification effect on the surface ground motion as well as the non-liquefied sites. The frequency content and the characteristics of the input motion may significantly affect the dynamic responses in liquefied sites. Site liquefaction amplified the pier top absolute displacements and internal forces at the pier bottom. Furthermore, liquefied sites modified the distribution of internal forces when compared with non-liquefied sites. The increases of the displacements may increase the possibility of pounding between the deck and the abutment or inducing collapsing, which close attention and consideration should be given to.

1 INTRODUCTION

One well-known study that is often cited in research on the theory of wave propagation in saturated porous media is that of Biot (1956), who introduces two elastic parameters which consider the compressibility of fluid and the elastic interaction between fluid and soil. The inertia and viscous interaction of fluid and soil are coupled into their equations of motion, which lays a foundation for the later study of dynamic response in saturated soil.

However, there are certain drawbacks associated with the use of Biot theory (Dobry, 1995). Practical engineering experience shows that there still has difficulty in measuring the coupling mass density of liquid-solid inertial in its dynamic equation. Later, many kinds of research have made related work, trying to improve and supplement Biot theory. It was not until the late 1960s that Rayleigh waves in isotropic saturated porous media have been first studied, ignoring the coupling inertial between the fluid and solid, and discussed the propagation velocity equation of Rayleigh waves in porous, elastic and saturated solids (Jones, 1961; Deresiewicz et al., 1962). In recent years, an effort has been made to analyze the effect of the parameters such as porosity and permeability under the consideration of replacing the classical Terzagh effective stress with the effective stress of porous media (Li et al., 2003). Based on Biot theory, it is found that the stress distribution between solid and fluid is affected by excitation frequency and permeability considering harmonic loading and vertical vibration (Halpern et al., 2010). Additionally, the elastic wave equation under the fluid-solid coupling effect was derived by assuming that the voids in saturated soil layers are uniformly distributed and interconnected (Chen et al., 1987). It has been shown that the effect of soil permeability on the P wave is more significant than that of S wave. The theory avoids the defects of Biot theory which is of practical value.

In order to solve the problems of the initial and final solutions of the transverse deformation of the cylinder by numerical method, Biot's theory has been applied in a saturated elastic semi-infinite space (Apirathvoraku et al., 1980). Many researches have been made progress so far based on Biot's theory (Li et al., 2004; Zeng et al., 1999; Philippacopoulos, 2014). Based on the centrifuge test, the p-y time history of the equivalent pile foundation is obtained and the

dynamic responses of pile foundations in liquefied sites are also obtained (Wilson et al., 2000). Additionally, some researches have revealed that the pore water pressure in saturated soil has a significant effect on the stiffness and damping of pile foundation (Yao et al., 2004) and the seepage rate of soil will affect the stiffness of the structure (Wang et al., 2003; Maeso et al., 2005).

However, the research on the dynamic response of foundation in the saturated soil started later in China. The saturated soil is considered as unidirectional medium, which is subject to a number of potential methodological weaknesses, such as its blindness and randomness (Gu et al., 2015). For offshore bridges, the geological environment of the pile foundation is in the seawater immersion for a long time, and the soil is basically under saturation state. The influence of liquefaction of saturated soil on pile foundations cannot be ignored. For this purpose, a water-soil-bridge system was adopted for study and investigating the responses under three seismic scenarios.

2 OVERVIEW OF THE BRIDGE STUDIED

As shown in Figure 1, a three-span offshore girder bridge with a continuous unit of 3x40 m was adopted. The pier immersion depth was 10.2 m. The superstructure featured a pre-stressed concrete with 7 pieces of T shape beam with a strength grade of C50 (50MPa). The pier adopted the double columns and solid circular section. Diameter and the height of piers were 2 m and 17 m respectively with a strength grade of C35 (35MPa). The pile foundation adopted double row piles, and the pile diameter was 1.8 m with a strength grade of C30 (30MPa). Foundation soils were in general composed of saturated soil ($v_s = 200\ m/s$), dense sand ($v_s = 248\ m/s$) of weathered rock ($v_s = 467\ m/s$). According to the type of bridge site, three seismic scenarios were selected according to the site classification as shown in Figure 3. The peak value of the accelerograms were scaled to 0.1 g, and the motion was imposed at the base horizontally.

3 MODELING OF THE SATURATED SOIL-BRIDGE SYSTEM

As shown in Figure 2, both the bridge and the near field soil were modeled in 3-Dimensions using the finite element program OpenSeeS. The deck, piers and piles were modeled with 3-Dimensional beam elements, and non-linear behavior of the pier columns have been taken into account. The bbarBrickUP element was adopted for the modeling of the saturated sand layer, which contained 3 translations and 1 pore water pressure degrees of freedom. Furthermore, PDMY was adopted for the constitutive model of the saturated sand (Yang et al., 2002), and the parameters used were shown in Table 1. A 150 m x 50 m soil domain was generated with constant depth of 50 m as well as the mesh size was 2.5 m x 2.5 m x 2.5 m. In order to be able to model soil-to-pile dynamic interaction, translational degrees of freedom between pile nodes and adjacent soil nodes were coupled. As for the boundary conditions, viscous-spring boundary elements with values depending on soil characteristics were

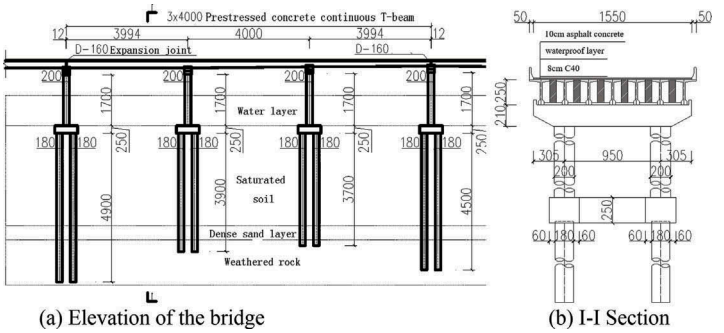

(a) Elevation of the bridge (b) I-I Section

Figure 1. Layout of the bridge configuration.

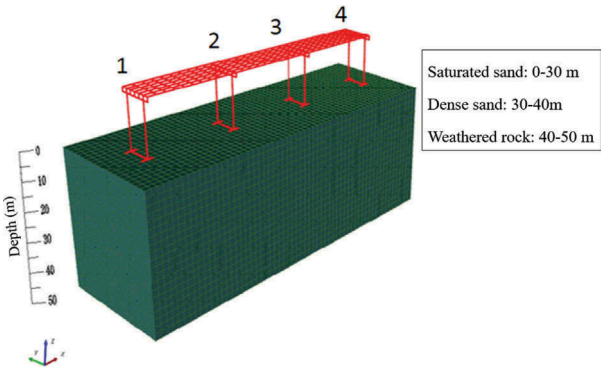

Figure 2. Finite element model of the saturated soil-bridge system.

Table 1. Parameters used for the constitutive model of saturated sand.

Parameter	value	Parameter	value
Density (kg/m^3)	1850	Volumetric shrinkage coefficient	0.07
Shear modulus at low strain rate (kPa, pr=80 kPa)	7.4×104	Coefficient of volume expansion 1	0.4
Bulk modulus (kPa, pr=80 kPa)	1.8×105	Coefficient of volume expansion 2	2.0
Friction angle (°)	33	Coefficient of liquefaction 1 (kPa)	10
Peak shear strain (pr=80 kPa)	0.1	Coefficient of liquefaction 2	0.01
Mean effective confining pressure (kPa)	80	Coefficient of liquefaction 3	1.0
Pressure correlation coefficient	0.5	Number of yield surface	20
Phase transformation angle (°)	27	Initial void ratio	0.7

*pr is the confining pressure for determining soil parameters.

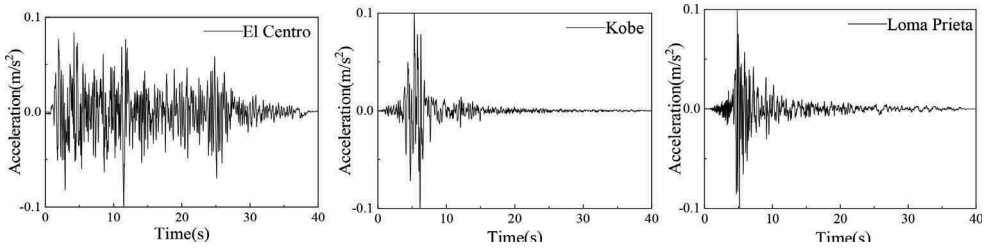

Figure 3. Three earthquake records used for the analysis.

implemented on the lateral surfaces of the soil domain in order to diminish reflections of waves (Liu et al., 2006). Rayleigh damping was also taken into account in this case.

The effect of wave force on piers was taken into account by Morison‘s additional mass method (Liu et al., 2008), which could be defined as the following equation:

$$M_W = (C_W - 1)\rho \frac{\pi D^2}{4} L \tag{1}$$

where M_W = additional mass at the pier nodes; C_W = dynamic water damping matrix;

Three different earthquake scenarios were investigated based on the records obtained from the El Centro, Kobe and Loma Prieta earthquakes as shown in Figure 3. The base excitations were obtained from appropriate deconvolution and baseline correction process, which were assumed as vertically propagating S-wave. As a result, site response was taken into account inherently by the structure of the 3-Dimensional soil domain, and no more analyses need to be performed for the site response.

4 ANALYSIS RESULTS

4.1 *The seismic site response*

Figures 4 and 5 showed the comparison of the seismic acceleration responses on the ground surface. In Figure 4, it was observed that the acceleration responses were more detrimental in non-liquefied site, in other words, liquefied site reduced the ground acceleration responses. Figure 5 showed the Fourier amplitudes of the accelerograms. It was shown, that in this case, liquefied site modified the frequency contents in a different way than non-liquefied site. The amplitudes decreased while the low frequency components increased in the liquefied site.

In order to investigate the liquefaction degree of soil, r_u was introduced and described as below:

$$r_{\mathrm{u}} = 1 - \frac{\sigma'}{\sigma'_0} \tag{2}$$

where σ' = effective stress; σ'_0 = initial effective stress. A value of this factor exceeds 0.6 represents the threshold of the liquefaction. The more this value is close to 1.0, the higher the liquefaction degree is. As could be seen in Figure 6, the site had been liquefied for the El Centro and Kobe earthquakes while slight liquefaction occurred for the Loma Prieta earthquake.

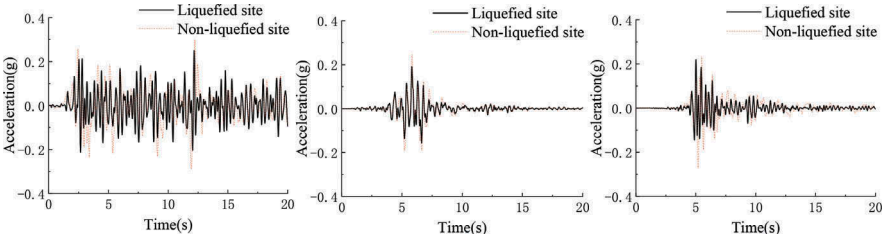

Figure 4. Accelerograms observed on the ground surface (liquefied site versus non-liquefied site) for the El Centro earthquake (left), the Kobe earthquake (middle) and the Loma Prieta earthquake (right).

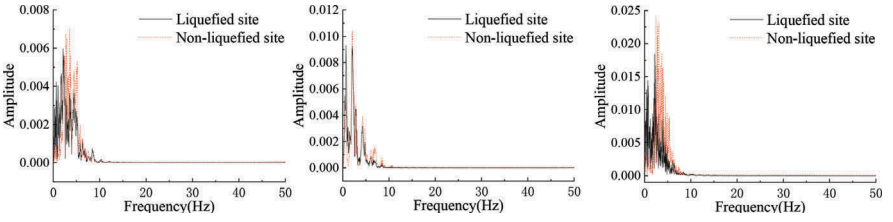

Figure 5. Fourier amplitude observed on the ground surface (liquefied site versus non-liquefied site) for the El Centro earthquake (left), the Kobe earthquake (middle) and the Loma Prieta earthquake (right).

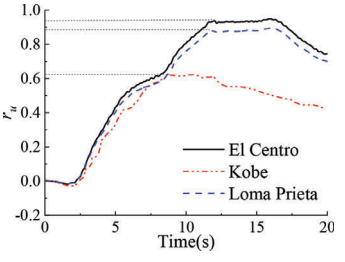

Figure 6. Pore water pressure ratio of the middle saturated sand in liquefied site.

4.2 *The seismic bridge response*

4.2.1 *Responses of the piers*

For an in-depth study of the problem, it was decided to focus on the relative response (i.e. pier top absolute displacements and pier base internal forces). As shown in Table 2, a value of the response ratio V exceeds1.0 represents the responses in the liquefied site is more unfavorable than the non-liquefied site. The displacement at the top of pier 3 was shown in Figure 7. It was observed that the peak displacement at pier top in liquefied site was larger than that in non-liquefied site. Table 2 showed the peak displacement comparison of the piers in the two sites. It was observed that the peak displacement of piers in liquefied sites increases significantly. For Loma Prieta earthquake, a maximum value of 1.19 was observed.

Figure 8 showed the comparisons of internal forces for Loma Prieta earthquake. At the beginning, the responses at the bottom of the liquefied site were smaller than those of the non-liquefied sites. One reason for this was the isolation effect of the liquefied sites, which reduced the response of the structure. However, with the development of liquefaction degree, the peak response value of the structure increased rapidly, which showed that the liquefied site had a significant impact on the seismic response of the structure.

4.2.2 *Responses of the piles*

According to the research on the structural damage of the liquefaction site after an earthquake, it is noted that the excessive displacement at the pile top is an important reason for the damage of a pile foundation. It was shown, that in Figure 9, the deformation of the liquefied site led to a significant increase in the lateral deformation of the pile, especially at the top. The shear force of the two sites reached the maximum at the interface between the medium sand

Table 2. Comparison of peak displacement of pier top.

Seismic scenarios	Pier number	Peak displacement (mm)		V
		Liquefied site (mm)	Non-liquefied site (mm)	
El Centro	1	19.8	17.3	1.14
	2	24.3	20.6	1.18
	3	23.2	20.2	1.15
	4	20.1	18.2	1.10
Kobe	1	12.2	11.6	1.05
	2	15.4	14.1	1.09
	3	14.3	13.2	1.08
	4	11.8	11.1	1.06
Loma Prieta	1	16.2	14.8	1.09
	2	18.6	15.7	1.18
	3	17.5	14.7	1.19
	4	15.8	13.9	1.14

*Response ration V is defined as: $V = V_{Liquefied}/V_{Non-liquefied}$.

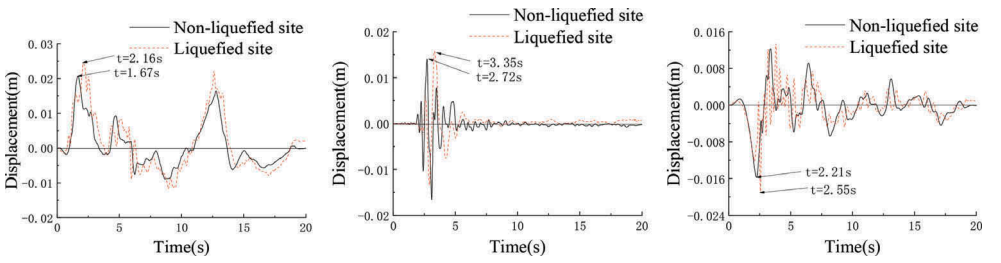

Figure 7. Comparison of displacement time histories at pier top.

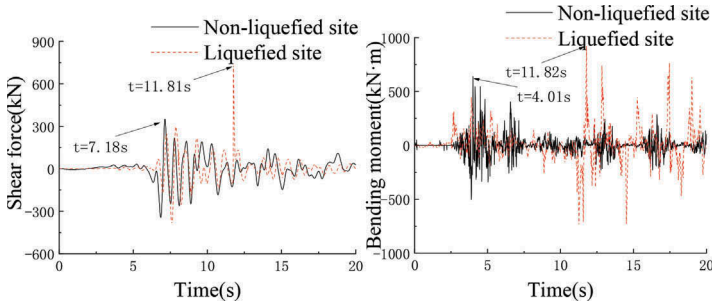

Figure 8. Comparison of internal force at pier bottom under Loma Prieta earthquake excitation.

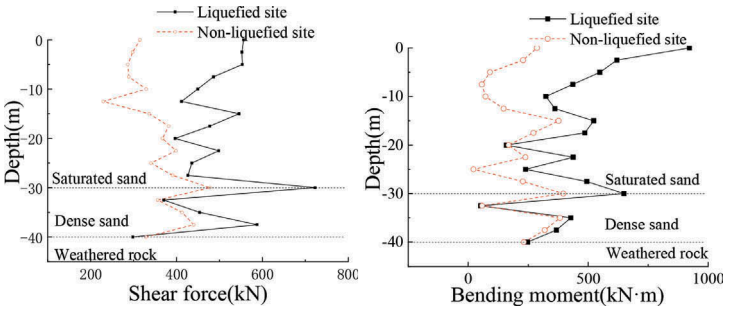

Figure 9. Peak internal forces along pile foundation under Loma Prieta earthquake excitation.

layer and the dense layer, and the maximum shear force of the liquefied site was obviously greater than that of the non-liquefied site. Because of the deformation of liquefied site, the maximum bending moment of pile foundation in liquefied site was observed at the top. In non-liquefied site, it occurred at the top of pile or at the interface of each soil layer. As illustrated in Table 3, the responses of shear force and bending moment increased up to 52% and 131% respectively for Loma Prieta earthquake. However, the responses of bending moment were similar in dense sand layer. Table 3 showed the comparison of maximum displacement and peak internal forces along the pile foundation. The definition of liquefaction coefficient V in the table was the same as that mentioned above. V_D, Vs and V_M were liquefaction coefficients of displacement, shear force and bending moment respectively. It was observed that the values in liquefied site were significantly higher than that in the non-liquefied site. The maximum liquefaction coefficients of displacement, shear force and bending moment were 2.82, 1.77 and 2.31 respectively for Loma Prieta earthquake.

4.2.3 *Responses of the beam*

In order to investigate the effect of site liquefaction on the beam, Table 4 gave the comparison of the peak horizontal displacement at the ends of the beam in the two sites. It was observed that

Table 3. Comparison of maximum displacement and peak internal force of pile foundation.

Seismic scenario	Site	Displacement (mm)	Shear force (kN)	Bending moment (kN·m)	V_D	V_S	V_M
El Centro	Liquefied	12.62	672.01	1435.16	1.98	1.77	1.61
	Non-liquefied	6.35	379.55	893.37			
Kobe	Liquefied	6.83	570.65	1060.52	1.25	1.32	1.56
	Non-liquefied	5.46	430.03	679.03			
Loma Prieta	Liquefied	10.12	724.83	929.79	2.82	1.52	2.31
	Non-liquefied	3.58	475.68	401.23			

Table 4. Comparison of peak displacement at the ends of the beam.

Seismic scenario	Position	Non-liquefied (cm)		Liquefied (cm)		Ratio	
		Left direction	Right direction	Left direction	Right direction	Left direction	Right direction
El Centro	Left end	10.93	17.31	9.51	24.58	0.87	1.42
	Right end	11.07	17.32	11.40	23.38	1.03	1.35
Kobe	Left end	5.38	5.73	5.06	6.99	0.94	1.22
	Right end	5.72	5.08	4.46	5.89	0.78	1.16
Loma	Left end	11.82	15.03	12.53	21.49	1.06	1.43
Prieta	Right end	11.88	15.05	14.37	23.78	1.21	1.58

*The ratio in the table is defined as the ratio of the liquefied over the non-liquefied.

liquefied site significantly amplified the displacement at the ends of the beam. The maximum displacement under Loma Prieta earthquake magnifies 1.58 times, which may lead to the risk of pounding or falling of superstructure and do damage to the superstructure or abutment. Therefore, in the seismic design of bridges in liquefaction sites, consideration should be taken to retain sufficient expansion joint space or limiting measures between beams or beam and abutment.

5 CONCLUSIONS

This study addressed the problem of the dynamic response of the bridge considering site liquefaction by comparing with the dynamic response of the non-liquefaction site. The conclusions drawn can be summarized as follows:

1. The displacement response of the pier increases in the liquefied site and the pier top absolute displacements showed a time delay compared with the non-liquefied site. The time histories of the internal forces at the bottom of the pier were obviously different in the two sites. The influence of liquefaction on the shear force at the pier bottom was greater than that of bending moment.
2. Compared with the site without liquefaction, the lateral deformation of pile foundation significantly increased in the liquefied site, especially at the top of the pile. For the shear force along the pile foundation, the maximum value of the two sites was at the interface between the saturated sand layer and the dense sand layer, and the maximum responses of the liquefied site were obviously greater than that of the non-liquefied site. For pile bending moment, the maximum responses mainly appeared at the top of the pile in the liquefied site, but it may occur at the pile top or at the interface of soil layers in non-liquefied site.
3. For the displacements at the ends of the beam, the peak displacement magnified 1.58 times in liquefied site, which may lead to the risk of pounding or falling of superstructure, resulting in damage of beam or abutment. Along these lines, close attention and consideration should be given to the seismic design in liquefied sites.

REFERENCES

Apirathvoraku, V. & Karasudhi, P. 1980. Quasi-static bending of a cylindrical elastic bar partially embedded in a saturated elastic half-space. *International Journal of Solids & Structures* 16: 625-644.

Arulmoli, K., Muraleetharan, K.K. & Hossain M.M., et al. 1992. Verification of liquefaction analyses by centrifuge studies, laboratory testing program: soil data report. CA: The Earth Technology Corporation.

Biot, M.A. 1956. Theory of Deformation of a Porous Viscoelastic Anisotropic Solid. *Journal of Applied Physics* 27: 459-467.

Chen, L., Wu, S. & Zeng, G. 1987. Propagation of elastic waves in water-saturated soils. *Acta Mechanic Sinica* 3: 92-100.

Deresiewicz, H. & Rice, J.T. 1962. The effect of boundaries on wave propagation in a liquid-filled porous solid-III: Reflection of plane waves at a free plane boundary (General Case). *Journal of Laboratory & Clinical Medicine* 53: 495-498.
Dobry, R. 1995. Centrifuge modeling of liquefaction effects during earthquakes. *Earthquake Geotechnical Engineering* 3: 1291-1324. Rotterdam: Balkema.
Gu, Y., Zhuang, S.M. & Zhuo, W.D., et al. 2015. Analysis of nonlinear seismic response of subway station considering saturated soil. *Rock & Soil Mechanics*. 36(11): 3243-3251.
Halpern, M.R. & Christiano, P. 2010. Steady-state harmonic response of a rigid plate bearing on a liquid-saturated poroelastic halfspace. *Earthquake Engineering & Structural Dynamics* 14: 439-454.
Jones, J.P. 1961. Rayleigh waves in a porous, elastic, saturated solid. *Journal of the Acoustical Society of America* 33: 959-962.
Li, P.C., Kong, X.Y. & LU, D.T. 2003. Mathematical modeling of flow in saturated porous media on account of fluid-structure coupling effect. *Journal of Hydrodynamics* 18: 419-426.
Liu, G.L. & Song, E.X. 2006. Visco-elastic transmitting boundary for numerical analysis of infinite saturated soil foundation. *Chinese Journal of Geotechnical Engineering* 28: 2128-2133.
Liu, J.B., Gu, Y. & Du, Y.X. 2006. Consistent viscous-spring artificial boundaries and viscous-spring boundary elements. *Chinese Journal of Geotechnical Engineering* 28: 1070-1075.
Liu, Z.Y., Li, Q. & Zhao, C.H. 2008. Earthquake-induced added hydrodynamic pressure on circular hollow piers in deep water. *Journal of Southwest Jiaotong University* 2: 200-206.
Maeso, O., Aznárez, J.J. & GarcíA, F. 2005. Dynamic impedances of piles and groups of piles in saturated soils. *Computers & Structures* 83: 769-782.
Philippacopoulos, A.J. 2014. Axisymmetric vibration of disk resting on saturated layered half-space. *Journal of Engineering Mechanics* 115: 2301-2322.
Qiang, L.I., Wang, K.H. & Xie, K.H. 2004. Study on resistance factor of saturated soil caused by longitudinal vibration of pile. *Chinese Journal of Geotechnical Engineering* 26: 679-683.
Wang, J.H., Zhou, X.L. & Lu, J.F. 2003. Dynamic response of pile groups embedded in a poroelastic medium. *Soil Dynamics & Earthquake Engineering* 23: 53-60.
Wilson, D.W., Boulanger, R.W. & Kutter, B.L. 2000. Observed seismic lateral resistance of liquefying sand. *Journal of Geotechnical & Geoenvironmental Engineering* 126: 898-906.
Xie, L., Han, B. & Xu, Z., et al. 2014. GPU powered high-performance computing method for the analysis of large-scale structures based on OpenSees. *Journal of Information Technology in Civil Engineering & Architecture* 6(5):22-25.
Xu, P.J. 2011. Seismic response analysis and simplified analysis method of bridge pile foundation in liquefiable ground. Harbin: Harbin Institute of Technology.
Yang, Z. & Elgamal, A. 2002. Influence of permeability on liquefaction-induced shear deformation. *Journal of Engineering Mechanics* 128: 720-729.
Yao, S., Kobayashi, K. & Yoshida, N., et al. 2004. Interactive behavior of soil-pile-superstructure system in transient state to liquefaction by means of large shake table tests. *Soil Dynamics & Earthquake Engineering* 24: 397-409.
Zeng, X. & Rajapakse, R.K.N.D. 1999. Dynamic axial load transfer from elastic bar to poroelastic medium. *Journal of Engineering Mechanics* 125: 1048-1055.
Zhang, R., Gu, B. & Shi, Z. 1997. Study on foundation liquefaction failure and critical pore water pressure of isolation. *Engineering Investigation* 2: 5-7.
Zienkiewicz, O.C. & Shiomi, T. 2010. Dynamic behavior of saturated porous media, the generalized Biot formulation and its numerical solution. International Journal for Numerical & Analytical Methods in Geomechanics 8: 71-96.